



Lipid-lowering treatment in a rabbit model of atherosclerosis: a vessel wall magnetic resonance imaging study

Yejun Wu^{1^}, Fangbing Li¹, Yilin Wang¹, Tianxiang Hu¹, Lianbo Gao²

¹Department of Radiology, The Fourth Affiliated Hospital of China Medical University, Shenyang, China; ²Department of Neurology, The Fourth Affiliated Hospital of China Medical University, Shenyang, China

Contributions: (I) Conception and design: Y Wu, L Gao; (II) Administrative support: L Gao; (III) Provision of study materials or patients: Y Wu, L Gao; (IV) Collection and assembly of data: F Li, Y Wang, Y Wu; (V) Data analysis and interpretation: F Li, Y Wang, T Hu, Y Wu; (VI) Manuscript writing: All authors; (VII) Final approval of manuscript: All authors.

Correspondence to: Lianbo Gao. Department of Neurology, The Fourth Affiliated Hospital of China Medical University, 4 Chongshan Road, Huanggu District, Shenyang 110032, China. Email: Gaolianbo_CMU4H@163.com.

Background: Vessel wall magnetic resonance imaging (VWMRI) is currently one of the best imaging techniques for the non-invasive evaluation of intracranial atherosclerotic lesions. However, it is still impossible to obtain pathological specimens of intracranial atherosclerotic plaques *in vivo*. The establishment of experimental animal models of atherosclerotic lesions similar to those of humans could solve this deficiency.

Methods: A model of abdominal aortic atherosclerosis in New Zealand white rabbits was established using abdominal aortic balloon dilatation combined with high-fat fodder. The pathological results were used as the reference standard for the successful establishment of the animal model. The rabbits with abdominal aortic atherosclerosis were randomly divided into the lipid-lowering treatment and the normal-fodder control groups. VWMRI and blood biochemical examinations were performed at 4, 12, and 24 weeks, and the radiologic-pathologic correlations were established.

Results: A rabbit abdominal aortic atherosclerosis model was established using balloon dilatation followed by high-fat fodder for 8 weeks. The lipid-lowering treatment reduced the plaque lipid core volume and decreased the plaque burden. However, it did not change plaque distribution, shape, or reverse vascular remodeling. Our pathological findings suggest that the lipid-lowering treatment reduced intraplaque macrophages but did not alter microvascular density.

Conclusions: VWMRI accurately assessed the morphological changes of the plaques before and after the lipid-lowering treatment, and the results support the pathology results. VWMRI could be useful in experimental studies on the pathogenesis, diagnosis, and treatment of atherosclerotic lesions.

Keywords: Vessel wall magnetic resonance imaging (VWMRI); atherosclerosis; rabbit; lipid-lowering treatment

Submitted Feb 21, 2022. Accepted for publication Mar 30, 2022.

doi: 10.21037/atm-22-1263

View this article at: <https://dx.doi.org/10.21037/atm-22-1263>

Introduction

Atherosclerosis is a vascular wall disease in the systemic arterial system, which can lead to arterial wall thickening, sclerosis, and luminal narrowing (1,2). Intracranial atherosclerotic

lesions are among the most important causative factors of ischemic stroke in Asians (3). Atherosclerotic plaque formation is an inflammatory process of the arterial intima, and it is accompanied by lipid deposition, foam cell formation, and

[^] ORCID: 0000-0003-1936-5002.

vascular smooth muscle cell migration (4). Treatment options for atherosclerotic lesions include statin interventions and healthy lifestyle changes.

Vessel wall magnetic resonance imaging (VWMRI) is currently one of the best imaging techniques for the non-invasive evaluation of intracranial atherosclerotic lesions (5). VWMRI had high spatial resolution and could directly image the vessel wall and lumen by suppressing blood signals, and it can identify distinct morphologic and enhancement patterns of atherosclerosis to provide important information about ischemic stroke etiology (6). The current expert consensus on technical specifications for VWMRI includes (I) high spatial resolution; (II) multiplanar 2D and 3D imaging; (III) multiple tissue-weighted sequences; (IV) suppression of blood and cerebrospinal fluid (7). VWMRI of intracranial atherosclerotic plaque typically demonstrates arterial wall thickening. However, as it is still impossible to obtain pathological specimens of intracranial atherosclerotic plaques *in vivo*, there is a lack of pathological findings to support intracranial arterial plaque images (8). The establishment of experimental animal models of atherosclerotic lesions similar to those of humans could solve this deficiency.

Rabbits are widely used in human atherosclerosis studies (9,10). Because of their unique lipoprotein metabolic profile and high sensitivity to a cholesterol diet, the lipid metabolism of rabbits is highly similar to that of humans, and the rabbit atherosclerosis model has provided many insights into the pathogenesis and development of human atherosclerosis (10).

In this study, we constructed a rabbit abdominal aortic atherosclerosis model and used VWMRI to analyze the imaging changes of rabbit abdominal aortic atherosclerotic lesions after treatment with atorvastatin and compared them to the pathological findings. Our innovation was that we continuously assess plaque changes at each treatment time point in experimental animals *in vivo*. We hypothesized that the VWMRI results would have good accord with the pathological results in evaluating rabbit abdominal aortic atheromatous plaques. We present the following article in accordance with the ARRIVE reporting checklist (available at <https://atm.amegroups.com/article/view/10.21037/atm-22-1263/rc>).

Methods

Animal model and feed

This experiment was performed under a project license (No.

EC-2019-KS-016) granted by the ethics committee of The Fourth Affiliated Hospital of China Medical University, in compliance with Chinese guidelines for the care and use of animals. A total of 40 5-month-old male New Zealand white rabbits weighing 2.5 ± 0.3 kg (Yu Dao Experimental Animal Breeding Co, Tianjin, China) were continuously housed at the School's animal care facilities (feeding environment: clean grade; temperature: 22 ± 1 °C; humidity: 45–55%; 12 h/12 h light–dark cycle; separate cage feeding, free water intake). The experiment lasted about 8.5 months (about 35 weeks) and was mainly divided into 2 parts. In Part 1, a high-fat diet combined with abdominal aortic balloon dilation was used to establish the rabbit abdominal aortic atherosclerosis model. In Part 2, atorvastatin was used to treat abdominal aortic atherosclerosis in the rabbits, and an image-pathological control was established.

First, the rabbits were randomly divided into the experimental group (n=34) and the control group (n=6). All the rabbits were fed normal fodder for 1 week and were tested for serum lipids and VWMRI to establish baseline reference standards.

Second, the rabbits in the experimental group were gradually fed with high-fat fodder for 2 weeks (the proportion of high-fat fodder was gradually increased from 50% to 100%, and the daily diet of each rabbit was 160 g of fodder), and an abdominal aortic balloon dilation was performed. The high-fat fodder was continued for 8 weeks after the operation to establish the rabbit model of abdominal aortic atherosclerotic plaque. Rabbits in the control group were fed normal fodder (a 160 g daily diet for each rabbit) for 2 weeks before the sham operation and were fed a normal diet for 8 weeks after the operation. Lipid testing and VWMRI were performed in both the experimental and control groups at postoperative weeks 4 and 8. Next, 3 rabbits in each group were randomly humanely killed for radiologic-pathologic correlation. The pathological results were used as a criterion to assess the success of the modeling, and if the modeling was successful, we proceeded to the next step of the experiment.

Third, the successfully modeled rabbits were randomly divided into the lipid-lowering and normal-fodder groups. The lipid-lowering group received fodder containing atorvastatin. The normal-fodder group received normal fodder. The rabbits in both groups underwent lipid testing and VWMRI at weeks 4, 12, and 24 after feeding, and the rabbits were randomly humanely killed at each testing time point for the radiologic-pathologic correlation.

The experimental fodder included normal fodder (alfalfa



Figure 1 Digital subtraction angiography image of rabbit abdominal aortic balloon dilatation angioplasty. The arrow indicates the dilated balloon.

meal 32%, cornmeal 5%, barley meal 30%, bean cake meal 15%, hay 15%, and inorganic salt and vitamin additive 3%), high-fat fodder (1% cholesterol, 5% fatty acid glycerides, 5% egg yolk powder, and 89% normal fodder), lipid-lowering fodder (atorvastatin 3 mg per 100 g of fodder, and the rest of the ingredients were normal fodder).

Rabbit abdominal aortic balloon dilation

The New Zealand rabbits were anesthetized with xylazine hydrochloride (Best Biologicals, Changsha, China) at a 0.2 mL/kg dose by injection into the marginal ear vein. The right femoral artery of the rabbit was used as the punctured artery. A guidewire was used to guide a 4 mm × 14 mm balloon (Cook Medical, Bloomington, USA) into the rabbit's abdominal aorta. Digital subtraction angiography (DSA) was then performed to determine the balloon position. The balloon was then dilated for 5 seconds and contracted for 20 seconds, and this was repeated 5 times to complete the rabbit's abdominal aortic endothelial injury (see *Figure 1*). The catheter was then removed, and the incision was sutured.

Rabbit MRI scanning protocol

After the rabbits were entirely anesthetized with xylazine

hydrochloride (0.2 mL/kg IV) in accordance with the experimental requirements, intravenous access was established in the rabbit's marginal ear vein. A 3.0 T magnetic resonance imaging (MRI; GE Discovery MR750; Milwaukee, WI, USA) with a knee coil was used for the scanning protocol, which included 3-dimensional (3D) time-of-flight (TOF) magnetic resonance angiography (MRA) and vessel wall imaging; the scanning parameters are shown in *Table 1*. The scanning area included the rabbit's abdominal aorta to the level of the bilateral iliac arteries. Gadobetidium glucosamine (0.5 mL; Modis, Shanghai Borealco Pharmaceuticals) was injected by hand at the ear margin vein with a flow rate of 0.02 mL/s. Delayed enhancement scans were performed 5 minutes after the contrast injection.

Definition of different features of VWMRI

Plaque burden: The lumen area and vessel area were measured at the narrowest vessel of the lesion. The plaque burden was calculated using the following formula: $(\text{vessel area} - \text{lumen area}) / \text{vessel area} \times 100\%$. The remodeling rate was defined as the ratio between the vascular area at the plaque and the vascular area proximal to the plaque (RR). Positive remodeling was indicated by an RR >1.05, negative remodeling by an RR 0.95, and no remodeling by an RR between 0.95 and 1.05 (11,12). The following formula was used to calculate the eccentricity index: $(\text{maximum vessel wall thickness} - \text{minimum vessel wall thickness}) / \text{maximum vessel wall thickness}$. The eccentricity index was used to evaluate the shape of the plaque. If the eccentricity index is ≥ 0.5 , it is eccentric vessel wall thickening; otherwise, it is centripetal (annular) vessel wall thickening (13). The signal of the rabbit abdominal aorta adjacent to the paraspinal muscle was used as a reference standard, and the plaque signal was classified as hypo-intensity, iso-intensity, or hyper-intensity (14).

Image analysis

The image quality of the VWMRI was reviewed by a radiologist. Based on the clarity of the vessel wall structure in the assessed imaging sequence, the image quality was then categorized into three levels: Level 1 is non-diagnostic, level 2 is not acceptable for diagnostic purposes, and level 3 is sufficient for diagnostic reasons (15). Second, 2 other radiologists independently measured and evaluated the VWMRI images using a blinded method according to the

Table 1 VWMRI protocol with a GE Discovery 3.0T MRI

Sequence	TR (ms)	TE (ms)	NEX	Slice thickness (mm)	FOV (cm)	Flip angle	Matrix size	Scanning time
3D TOF-MRA	23	2.5	3	2	16	18	256×256	08:22
3D CUBE T1WI	1,140	14	1	0.8	18	–	256×256	06:38
3D CUBE PDWI	1,500	35	1	0.8	18	–	256×256	03:25
3D CUBE T2WI	1,500	90	2	0.8	18	–	256×256	03:41
3D CUBE T1WI with contrast agent	1,140	14	1	0.8	16	–	256×256	06:38

VWMRI, vessel wall magnetic resonance imaging; GE, General Electric Company; 3D, three dimensional; TOF, time-of-flight; MRA, magnetic resonance angiography; CUBE, variable-flip-angle turbo-spin-echo; T1WI, T1-weighted imaging; PDWI, proton density-weighted imaging; T2WI, T2-weighted imaging; TR, repetition time; TE, echo time; NEX, number of excitations; FOV, field of view.

above criteria. The histological information of all the rabbits was not visible during the measurement and evaluation. All the measurements were performed on a GE workstation. The lumen was manually outlined on T1-weighted imaging (T1WI), and the outer wall of the vessel was drafted on T2-weighted imaging (T2WI). The GE workstation automatically calculated the lumen and vessel areas.

Histological processing and measurement of rabbits

The rabbits were euthanized by an overdose of an anesthetic injection (Xylazine hydrochloride, 2 mL/kg), and the abdominal aorta to the bilateral iliac arteries was removed, fixed with 4% paraformaldehyde, and sectioned for staining. Pathological staining included: hematoxylin-eosin (HE) staining and immunohistochemical (CD31/CD68, GTX34492/GTX34542, Genetex, USA) staining.

Additionally, 4 consecutive specimen segments of abdominal aortic lesions were removed from the rabbits with the left renal artery as the reference point, and the images of the pathological sections were counted and measured using Image J (version 1.53e, National Institutes of Health, USA). The pathological section was independently measured and evaluated by 2 doctors using a blinded method.

The vascular area, lumen area, and vessel wall area of the rabbit's abdominal aorta were measured on a 40× field of view of the HE sections. In this study, 4 × 400× fields of view were randomly selected on each immunohistochemical (CD68/CD31) section. The plaque macrophage positive area ratio (positive staining area/total plaque area) and plaque neovascularization density (number of neovascularization microvessels/total plaque area) were calculated separately. The locations of the macrophages and neovascularization in the atheromatous plaques were also observed.

Rabbit serum lipoprotein concentration assay

An immune transmission turbidimetric method was used to measure serum triglyceride, total cholesterol, low-density lipoprotein cholesterol, and high-density lipoprotein cholesterol concentration.

Statistical analysis

All the statistical analyses were performed using statistical software (MedCalc v19.0.7; MedCalc Software 149 Ltd, Ostend, Belgium). The Shapiro-Wilk test was used to verify whether the continuous variables conformed to a normal distribution. The VWMRI images and pathological sections were re-evaluated by 1 of the 2 doctors 4 weeks later to assess interobserver agreement. Intra and interobserver agreement were evaluated using the intraclass correlation coefficient (ICC); an ICC >0.80 indicated good agreement; an ICC of 0.40–0.80 indicated fair agreement, and an ICC <0.4 indicated poor agreement. Serum test data, VWMRI measurements, and pathology section measurements for all groups at each testing time point were compared using the signed rank-sum test, Wilcoxon rank-sum test, paired *t*-test, or independent sample *t*-test. The agreement between the VWMRI and pathology section measurements was statistically evaluated using a Pearson coefficient correlation. A *P* value <0.05 was considered statistically significant.

Results

Changes in serum lipoproteins in rabbits in the control and experiment groups

There were no deaths in the control group. In the experimental group, 1 rabbit died from preoperative anesthesia, and

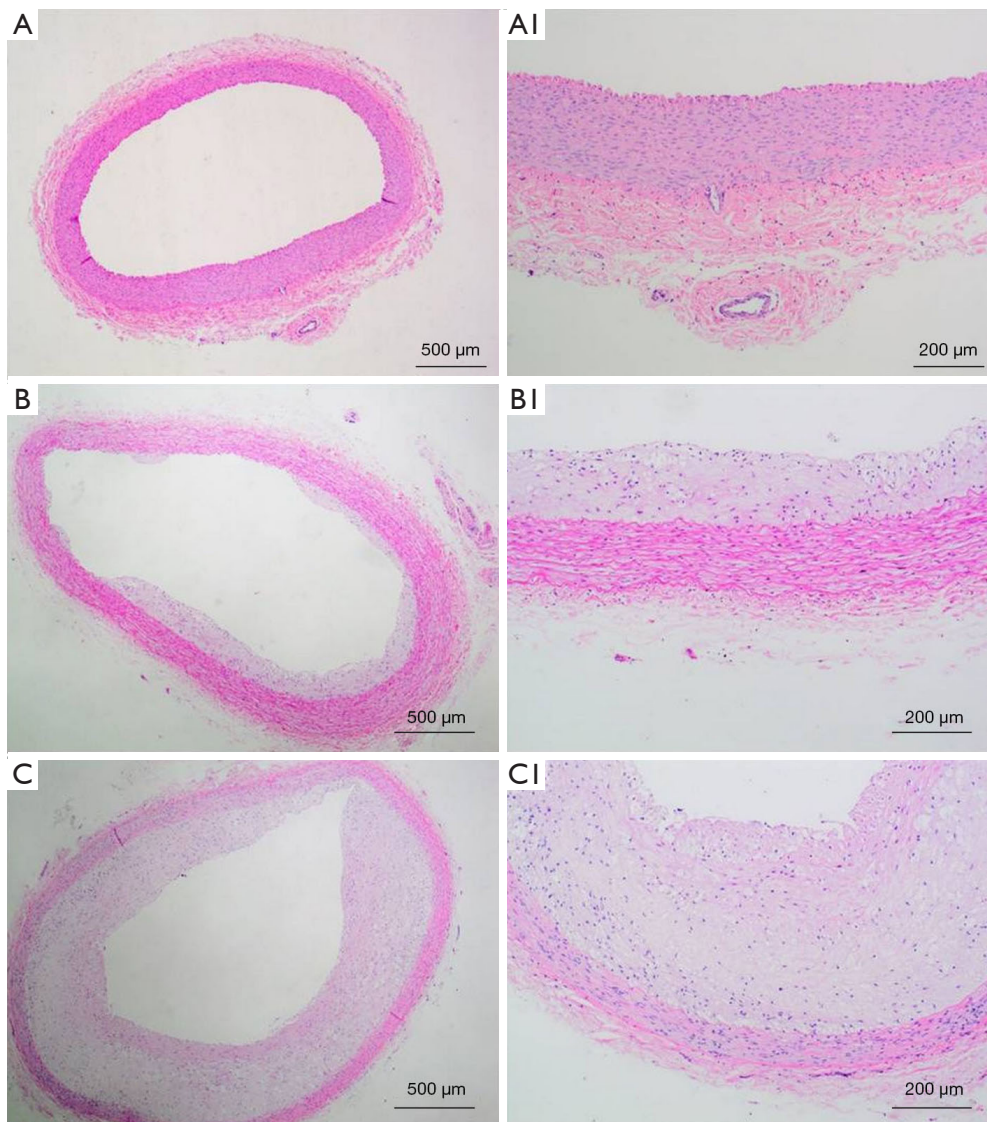


Figure 2 Pathological sections of the abdominal aorta of rabbits in the experimental group (baseline to 8 weeks). (A,A1) ($\times 40/\times 100$): HE staining of a rabbit's abdominal aorta before modeling (baseline). (B,B1) ($\times 40/\times 100$): HE staining of a rabbit's abdominal aorta at 4 weeks of modeling. (C,C1) ($\times 40/\times 100$): HE staining of a rabbit's abdominal aorta at 8 weeks of modeling. The lumen of the abdominal aorta gradually narrowed, the vessel wall gradually thickened, and multiple plaques appeared in the vessel wall. HE, hematoxylin-eosin.

4 died gradually during postoperative high-fat fodder feeding. The pathological results confirmed that the model rabbit with abdominal aortic atherosclerosis had been successfully established at the 8-week time point (see *Figure 2*).

The serum lipoprotein concentration of the rabbits in the experimental group increased significantly, while the serum lipoprotein concentration of the rabbits in the control group did not change significantly and was significantly lower than

that of rabbits in the experimental group (see *Table 2*).

Correspondence between VWMRI and pathological findings in the experimental and control groups

The pathological sections revealed that the vessel wall of the control rabbit abdominal aorta was smooth with a regular morphology, the inner membrane was smooth with only a single layer of endothelial cells arranged, and the middle

Table 2 Serum lipid concentrations in the experimental and control groups

Rabbit serum lipoprotein concentration (mmol/L)	Experimental group	Control group	P
Total cholesterol			
Baseline*	1.03±0.41	0.96±0.31	0.54
4 weeks [#]	9.87±1.38	1.16±0.13	0.00
8 weeks ^{&}	11.89±1.09	1.33±0.32	0.00
Triglyceride			
Baseline*	0.60±0.20	0.61±0.41	0.85
4 weeks [#]	3.52±0.83	0.69±0.06	0.00
8 weeks ^{&}	3.63±0.57	0.75±0.11	0.00
Low-density lipoprotein			
Baseline*	0.35±0.16	0.36±0.12	0.70
4 weeks [#]	6.52±1.01	0.50±0.19	0.00
8 weeks ^{&}	7.01±1.29	0.76±0.11	0.00
High-density lipoprotein			
Baseline*	0.15±0.05	0.16±0.02	0.49
4 weeks [#]	3.15±0.45	0.16±0.04	0.00
8 weeks ^{&}	3.56±0.32	0.13±0.02	0.00

*, experimental group n=34; control group n=6; [#], experimental group n=32; control group n=6; [&], experimental group n=29; control group n=6. VWMRI, vessel wall magnetic resonance imaging.

layer of the vessel was mainly smooth muscle cells. In the experimental group, the intima of the rabbit's abdominal aorta was unevenly thickened, with attached plaques and increased luminal stenosis. The plaque cap was unevenly thin and thick, and fibrous components were visible in the fibrous cap and myocardium.

The immunohistochemistry results also showed that macrophages and neovascularization gradually appeared in the rabbit abdominal aortic plaques following prolonged feeding on a high-fat diet. The new microvasculature was present in the fibrous cap on the plaque surface, at the base of the plaques, and partially in the lipid core. The macrophages were mainly clustered in the lipid core of the plaques (see *Figure 3*).

There were statistical differences in the density of neovascularization (7.12 ± 0.31 vs. 0.00 mm²; $P < 0.01$) and the positive macrophage area ratio (17.75 ± 5.12 vs. 0.00 ; $P < 0.01$) in the experimental group compared to the control group.

The VWMRI of the rabbit's abdominal aorta was essentially morphologically consistent with the pathological sections. The wall thickening and plaque distribution in the

experimental group's pathological sections corresponded well to those in the VWMRI (see *Figure 4*). The control group's VWMRI of the rabbit abdominal aorta showed a thin and smooth wall with uniform thinness, no lumen stenosis, and no vessel remodeling. The lumen displayed hypo-intensity, the vessel wall displayed intensity on T1WI and proton density-weighted imaging (PDWI) with no significant enhancement in the T1WI postcontrast sequence. The abdominal aorta wall was circumferentially or heterogeneously eccentrically thickened in the experimental group. The plaques showed iso-/hypo-intensity in T1WI and iso-/hyper-intensity in PDWI. Plaque enhancement was observed on a T1WI postcontrast sequence. The lumen was narrow with positive remodeling. The results of various vascular measurements in the abdominal aorta of the rabbits in the control and experiment groups are shown in *Table 3*.

Changes in serum lipoproteins in rabbits in the lipid-lowering and normal-fodder groups

The 29 rabbits with abdominal aortic atherosclerosis were

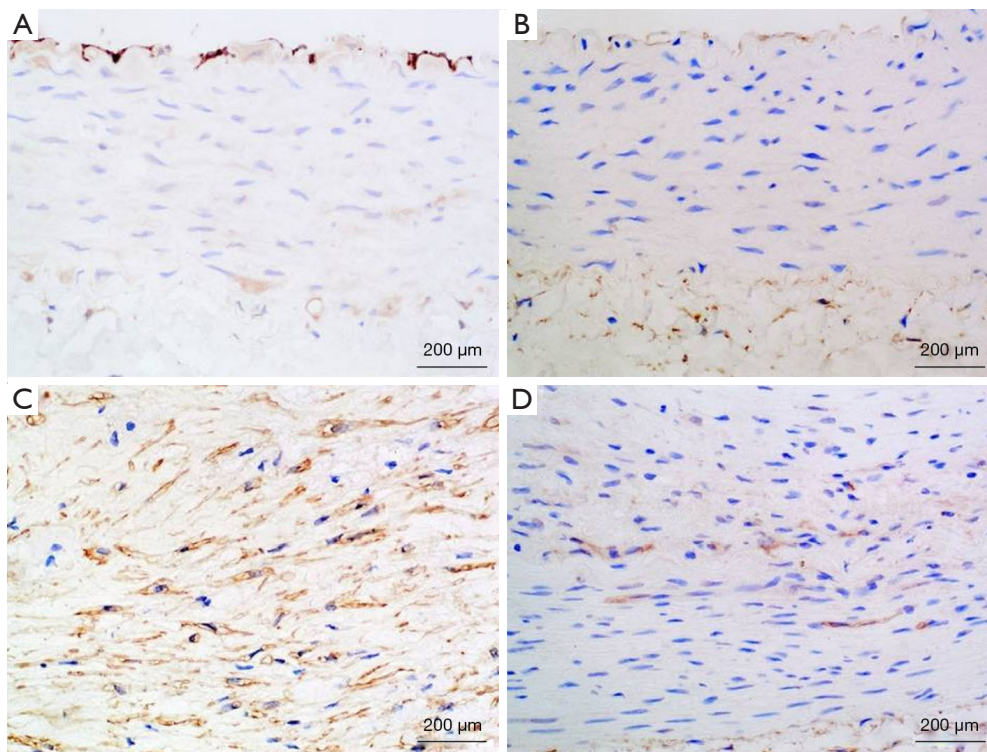


Figure 3 Immunohistochemical results of a rabbit abdominal aorta. The immunohistochemical methods showed no neovascularization distribution in the vessel wall of the CD31-labeled normal rabbit abdominal aorta (A), while neovascularization was present in the rabbit abdominal aortic atherosclerotic plaques (C). There was no macrophage distribution in the vascular wall of the CD68-labeled normal rabbit abdominal aorta (B), but macrophages were present in the atherosclerotic plaques of the rabbit aorta (D).

randomly divided into the lipid-lowering group (19 rabbits) and the normal-fodder group (10 rabbits) using a 2:1 ratio. During the treatment period, 3 rabbits died in the lipid-lowering group and 4 died in the normal-fodder group.

The serum lipoprotein concentrations of the rabbits in the lipid-lowering and normal-fodder groups are shown in *Table 4*. The serum lipoprotein concentrations of rabbits in the lipid-lowering group showed a significant decreasing trend. The serum lipoprotein concentration of rabbits in the normal-fodder group decreased slowly and to a lesser extent than that in the lipid-lowering group.

Correspondence between VWMRI and pathological findings in the lipid-lowering and normal-fodder groups

The results of various vascular measurements in the abdominal aorta of the rabbits in the lipid-lowering treatment group and the normal-fodder group are set out in *Table 5*. After 24 weeks of the lipid-lowering treatment, there were statistically significant differences in the changes

in the lumen area (2.59 ± 1.18 vs. 4.05 ± 0.69 mm²; $P < 0.01$) and the vessel wall area (15.55 ± 2.98 vs. 9.65 ± 1.23 mm²; $P < 0.01$). The mean decrease in the plaque burden in the abdominal aorta of the rabbits was about 17.85% ($85.73\% \pm 7.28\%$ vs. $70.43\% \pm 5.32\%$; $P < 0.01$). There were no statistically significant changes in the abdominal aortic measurements of the rabbits in the normal-fodder group.

Pathological sections and VWMRI of the abdominal aorta of the rabbits in the lipid-lowering treatment group had approximately the same morphological appearance (see *Figure 5*). The reduction of plaque volume was mainly reflected in reducing the lipid core within the plaque, and the thickness of the fibrous cap on the plaque surface increased. However, the lipid-lowering treatment did not reverse the vascular remodeling (1.53 ± 0.19 vs. 1.16 ± 0.23) and the distribution of the plaques (13 cases in the circumferential wall, 1 case in the left wall, and 2 cases in the right wall). Further, the model of wall thickening was not significantly altered.

No significant changes were observed in the normal feed

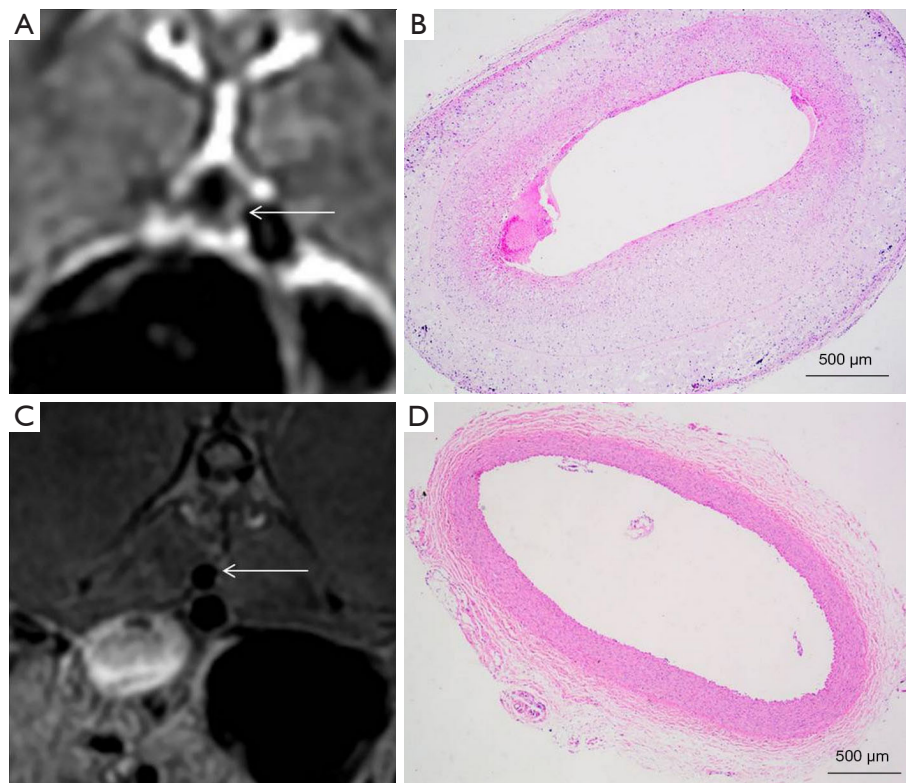


Figure 4 Experimental and control rabbit abdominal aorta radiologic-pathologic correlations. (A) 3D CUBE T1WI of the abdominal aorta of a rabbit in the experimental group. The arrow indicates plaque. (B) HE pathology section of the abdominal aorta of the same rabbit in the experimental group ($\times 40$). (C) 3D CUBE T1WI of the abdominal aorta of a rabbit in the control group. The arrow indicates the normal lumen. (D) HE pathology section of the abdominal aorta of the same rabbit in the control group ($\times 40$). 3D CUBE T1WI, three dimensional variable-flip-angle turbo-spin-echo T1-weighted imaging. HE, hematoxylin-eosin.

Table 3 Comparison of the control group and experimental group of the rabbit abdominal aorta by VWMRI and pathological section

	VWMRI	Pathological section	r (P)
Vascular area (mm^2)			
Control group	11.82 \pm 1.99	11.62 \pm 0.49	0.72 (0.01)
Experimental group	18.04 \pm 3.02	17.55 \pm 1.14	0.69 (0.02)
Intra and interobserver	0.97/0.96	0.95/0.93	–
Lumen area (mm^2)			
Control group	7.77 \pm 1.59	7.23 \pm 0.43	0.65 (0.03)
Experimental group	2.60 \pm 1.14	2.65 \pm 0.26	0.87 (0.00)
Intra and interobserver	0.98/0.93	0.97/0.94	–
Vessel wall area (mm^2)			
Control group	4.40 \pm 0.74	4.26 \pm 1.28	0.71 (0.03)
Experimental group	15.44 \pm 2.89	14.93 \pm 0.67	0.67 (0.02)
Intra and interobserver	0.99/0.97	0.98/0.98	–

Control group: n=6; Experimental group: n=3 (pathological section); n=29 (VWMRI). VWMRI, vessel wall magnetic resonance imaging.

Table 4 Serum lipid concentrations in the lipid-lowering and normal-fodder groups

Rabbit serum lipoprotein concentration (mmol/L)	Lipid-lowering group	Normal-fodder group	P
Total cholesterol			
Baseline [§]	11.89±1.45	11.89±1.09	0.87
4 weeks*	8.52±1.55	11.79±1.13	0.00
12 weeks [#]	3.32±1.75	6.37±1.21	0.00
24 weeks ^{&}	1.89±0.57	3.89±1.28	0.00
Triglyceride			
Baseline [§]	3.63±0.57	3.63±0.47	0.83
4 weeks*	2.38±0.75	3.37±0.29	0.00
12 weeks [#]	1.17±0.12	2.75±0.51	0.00
24 weeks ^{&}	1.07±0.19	2.08±0.55	0.00
Low-density lipoprotein			
Baseline [§]	7.01±1.35	7.01±1.29	0.89
4 weeks*	4.08±0.97	6.13±1.26	0.00
12 weeks [#]	1.76±1.03	4.53±1.37	0.00
24 weeks ^{&}	1.01±0.36	2.18±0.44	0.00
High-density lipoprotein			
baseline [§]	3.56±0.32	3.56±0.25	0.90
4 weeks*	1.86±1.10	3.63±0.27	0.00
12 weeks [#]	0.48±0.32	2.08±1.18	0.00
24 weeks ^{&}	0.38±0.11	0.78±0.14	0.00

[§], lipid-lowering group n=19, normal-fodder group n=10; *, lipid-lowering group n=18, normal-fodder group n=7; [#], lipid-lowering group n=17, normal-fodder group n=6; [&], lipid-lowering group n=16, normal-fodder group n=6.

group with atherosclerotic lesions in the abdominal aorta. VWMRI was used to evaluate the fibrous cap changes, but the histological structure was not as well displayed in VWMRI as it was in the pathological sections.

Compared to the baseline, the number of macrophages within the lipid core of the rabbit abdominal aortic plaques treated with lipid-lowering therapy for 24 weeks showed a progressive decrease (16.92±8.19 vs. 7.13±2.19; P<0.01), but there was no significant difference in the distribution and number of new microvessels in the plaques (6.79±0.24 vs. 6.51±0.21, P=0.81; *Figure 6*). After 24 weeks of lipid-lowering treatment, plaque enhancement on 3D CUBE T1WI postcontrast sequence was reduced compared to baseline. However, there was no significant statistical difference in the change of plaque enhancement degree between each treatment time point, so the changing trend

of plaque enhancement degree could not well reflect the gradual changes of macrophages and neovascularization in the plaque in pathological sections.

Discussion

Appropriate experimental animals are essential for basic research and clinical research on treatment and diagnosis. Rabbits were used as the experimental animals in this study for some reason. First, rabbits were the first animal model used to study human atherosclerosis. Second, rabbits have unique characteristics of lipoprotein metabolism and are highly sensitive to a cholesterol diet (16). Third, many characteristics of rabbit lipid metabolism make it particularly suitable for animal experiments related to the study of human lipoprotein metabolism and atherosclerotic

Table 5 Comparison of the lipid-lowering group and normal-fodder group of the rabbit abdominal aorta by VWMRI and pathological section

	Lipid-lowering group			Normal-fodder group		
	VWMRI	Pathological section	r (P)	VWMRI	Pathological section	r (P)
Vascular area (mm²)						
Pre-treatment [§]	18.14±3.12	17.62±0.59	0.81 (0.02)	17.94±3.13	17.49±0.47	0.72 (0.03)
4 weeks*	17.79±3.29	17.42±0.37	0.77 (0.01)	17.87±2.23	17.61±0.58	0.79 (0.02)
12 weeks [#]	14.23±1.81	14.78±0.25	0.75 (0.03)	17.69±3.15	17.62±0.37	0.85 (0.00)
24 weeks ^{&}	13.70±1.53	14.06±0.38	0.83 (0.02)	17.99±2.96	17.55±0.32	0.73 (0.03)
Intra and interobserver	0.95 (0.93)	0.97 (0.96)	–	0.94 (0.93)	0.97 (0.97)	–
Lumen area (mm²)						
Pre-treatment [§]	2.59±1.18	2.63±0.31	0.81 (0.01)	2.59±1.13	2.67±0.21	0.81 (0.01)
4 weeks*	2.60±0.38	2.63±0.38	0.88 (0.00)	2.66±1.30	2.78±0.24	0.80 (0.02)
12 weeks [#]	3.92±0.53	3.72±0.60	0.75 (0.03)	2.66±1.26	2.62±0.23	0.84 (0.00)
24 weeks ^{&}	4.05±0.69	3.69±0.51	0.71 (0.03)	2.67±1.27	2.76±0.44	0.83 (0.01)
Intra and interobserver	0.97 (0.96)	0.98 (0.98)	–	0.97 (0.96)	0.96 (0.96)	–
Vessel wall area (mm²)						
Pre-treatment [§]	15.55±2.98	15.09±0.74	0.70 (0.04)	15.34±3.01	14.82±0.65	0.69 (0.03)
4 weeks*	15.19±3.07	14.79±0.51	0.76 (0.02)	15.21±3.11	14.83±0.56	0.69 (0.04)
12 weeks [#]	10.31±1.48	11.03±0.67	0.65 (0.04)	15.03±2.91	14.91±0.33	0.83 (0.01)
24 weeks ^{&}	9.65±1.23	10.01±0.71	0.70 (0.03)	15.32±2.77	14.79±0.45	0.66 (0.04)
Intra and interobserver	0.93 (0.94)	0.95 (0.93)	–	0.94 (0.94)	0.95 (0.95)	–

[§], VWMRI (lipid-lowering group n=19, normal-fodder group n=10); pathological section (lipid-lowering group n=3, normal-fodder group n=3); *, VWMRI (lipid-lowering group n=16, normal-fodder group n=7); pathological section (lipid-lowering group n=3, normal-fodder group n=3); #, VWMRI (lipid-lowering group n=13, normal-fodder group n=4); pathological section (lipid-lowering group n=3, normal-fodder group n=3); &, lipid-lowering group n=10, normal-fodder group n=1. VWMRI, vessel wall magnetic resonance imaging.

characteristics (17). In Asian populations, atherosclerotic lesions involving the middle cerebral artery are widespread. Finally, similar to the lumen and diameter of the human middle cerebral artery, the lumen of the rabbit's abdominal aorta is straight and approximately 3–5 mm in diameter.

The main advantages of using rabbits to construct atherosclerosis animal models rather than other commonly used animal models, such as primates and pigs, include their easy maintenance and availability, low economic cost, and better suitability for interventional surgery and MRI examination (18,19). The rabbit abdominal aorta was chosen as the target vessel to construct an atherosclerosis model for the following reasons: the rabbit abdominal aorta is straight and easy to operate on, and the bilateral renal artery-opening is a good reference standard for localization. The rabbit's abdominal aorta is close to the spine, and its

MRI signal has good tissue contrast with the signal of the paraspinal muscles, which facilitates the observation of the signal characteristics of the rabbit's abdominal aorta. Further, the relatively long vascularity of the rabbit's abdominal aorta facilitates the construction of more atherosclerotic plaques.

Previous studies evaluating the therapeutic efficacy of atorvastatin in the treatment of abdominal aortic atherosclerosis in rabbits have generally classified atorvastatin treatment doses as low (1 mg/kg/day), standard (5 mg/kg/day), or high (10 mg/kg/day) (20,21). The incidence of adverse reactions and mortality in rabbits was significantly higher after treatment with high doses of atorvastatin. Low-dose atorvastatin has a good safety profile; however, the therapeutic efficacy of the drug is lower than that of standard-dose atorvastatin (21). Given

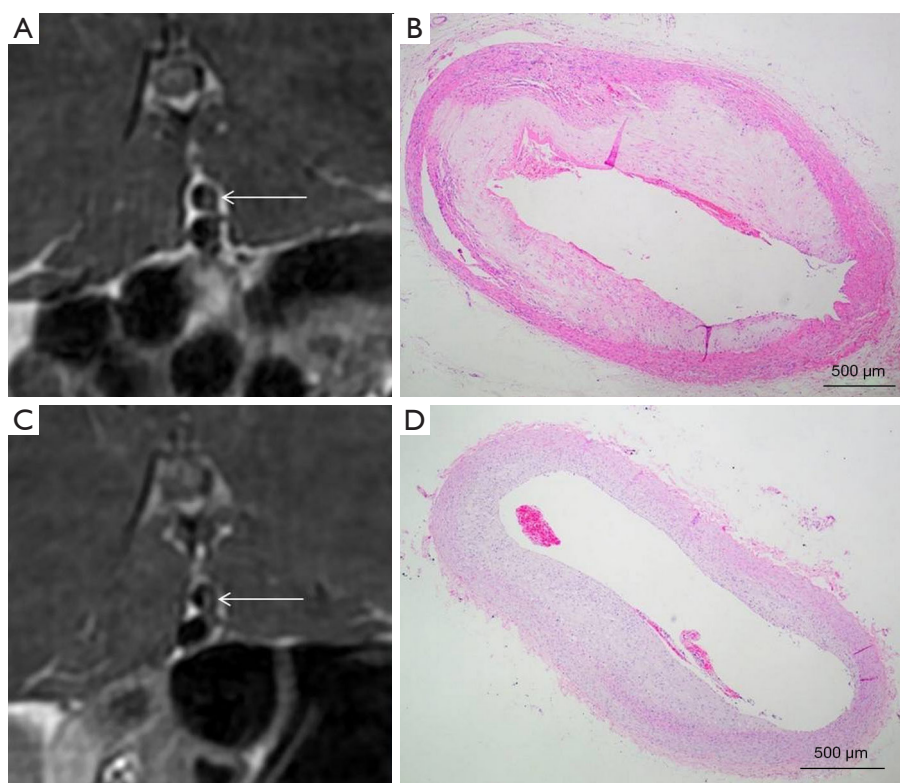


Figure 5 Radiologic-pathologic correlations of abdominal aortic plaque in rabbits after the lipid-lowering treatment. After 24 weeks of the lipid-lowering treatment, abdominal aortic plaque volume was reduced, and the degree of lumen stenosis was alleviated. (A) 3D CUBE T1WI of the abdominal aorta plaque of a rabbit before the lipid-lowering treatment. The arrow indicates plaque. (B) HE pathology section of the abdominal aorta plaque of the same rabbit ($\times 40$). (C) 3D CUBE T1WI of the abdominal aorta plaque of the same rabbit after 24 weeks of the lipid-lowering treatment. The arrow indicates plaque. (D) HE pathology section of the abdominal aorta of the same rabbit in the normal-fodder group ($\times 40$). 3D CUBE T1WI, three dimensional variable-flip-angle turbo-spin-echo T1-weighted imaging. HE, hematoxylin-eosin.

our long experimental period, to minimize the adverse reactions leading to rabbit mortality and consider the drug's therapeutic effect, we used a dose of atorvastatin that was between the low and standard dose for treatment. The rabbits in the lipid-lowering group ate 160 g of food per day, containing 4.8 mg of atorvastatin during the treatment period. The rabbits in the treated group did not die during the experiment due to adverse drug reactions, and the therapeutic effect of our atorvastatin dose was confirmed by the serum lipoprotein levels and VWMRI and pathology results. In this study, the serum lipoprotein concentration in the lipid-lowering group continued to decrease significantly, while the concentration only decreased slowly in the normal-fodder group. The main reason for this is the decrease in the number of lipoprotein receptors in spontaneous regression after the interruption of a high-

cholesterol diet, which increases the retention time of lipids in the blood circulation and increases the time it takes for plasma cholesterol return to normal levels.

Previously, the progression of atherosclerotic lesions was thought to be irreversible. However, the previous study demonstrated that the retraction of atherosclerotic lesions could occur (22). Reducing the lipid component of atherosclerotic plaques by intervening in factors affecting lipid efflux can directly lead to the out-migration or reduction of macrophages and a reduction in plaque volume (23). Similarly, our experimental study came to the conclusion that atorvastatin stabilizes and reverses atherosclerotic plaques. We assessed the atherosclerotic plaque changes by VWMRI with atorvastatin treatment. The reduction in the plaque burden was mainly reflected in the reduction of the lipid core in the plaque component.

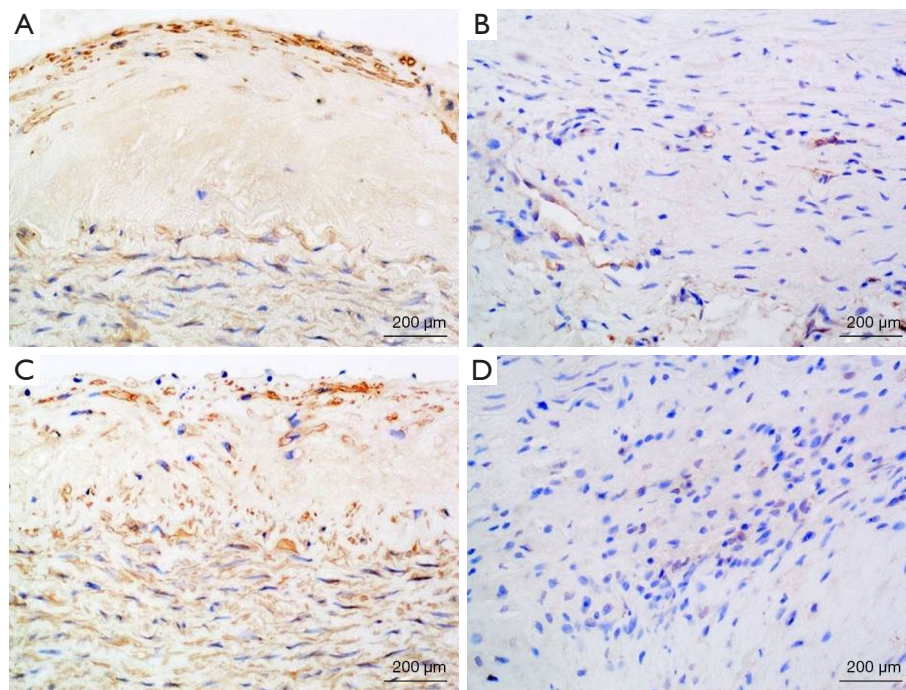


Figure 6 Immunohistochemistry results of the rabbit abdominal aorta after the lipid-lowering treatment. The immunohistochemical methods showed no significant difference in the distribution of CD31-labeled neovascularization in the rabbit abdominal aortic vessel wall after 24 weeks of the lipid-lowering treatment (A) before the lipid-lowering treatment; (C) after the lipid-lowering treatment. The immunohistochemical methods showed a decrease in the distribution of the CD68-labeled macrophages in the rabbit abdominal aortic vessel wall after 24 weeks of the lipid-lowering treatment (B) before the lipid-lowering treatment; (D) after the lipid-lowering treatment.

Atherosclerotic plaques are lipids, thrombotic material (platelets and fibrin), cellular material, and the connective tissue matrix. The main components exhibited on VWMRI were the lipid core and the fibrous cap on the surface. In relation to the plaque, 3D CUBE T1WI showed a significant overall plaque volume predominance, while 3D CUBE PDWI showed a significant fibrous cap predominance. The vulnerable plaques were highly correlated with ischemic stroke and stroke recurrence. The plaque enhancement with VWMRI may indicate plaques at risk of instability. A postmortem study found that neovascularity in middle cerebral artery (MCA) atherosclerotic plaque was associated with ipsilateral infarction (24). The plaque enhancement correlates with histologic findings of both inflammation and neovascularization.

During the modeling and treatment of atherosclerosis in rabbits, there was a discrepancy between the vascular values measured by the pathological sections and those measured by VWMRI. We analyzed the difference in measurements between the 2 methods because the abdominal aortic

specimens from rabbits were not stained immediately after sampling but were uniformly pathologically stained at the end of the study. The shrinkage of isolated specimens during fixation, dehydration, and embedding resulted in differences in the *in-vivo* tissue, and many measurements may have been underestimated. The absence of blood filling in isolated specimens of the rabbit's abdominal aorta, without the fixation and support of surrounding tissues, may have also contributed to the underestimation of the vascular measurements.

This study had some limitations. First, previous publications have used techniques such as dynamic enhancement magnetic resonance and positron emission computed tomography that can indirectly respond to vascular and macrophage changes in the plaques in experimental animals (25,26); however, due to the limitations of the experimental conditions, the present study used delayed enhancement scans for VWMRI, which did not reflect the changes of intraplaque neovascularization and macrophages during the treatment. Second, while the rabbit's abdominal aorta is close to the spine, the artifacts generated by the

breathing motion of the rabbit are still a key factor affecting the image quality of the rabbit's abdominal aortic vessel wall. Because of the wide range and high spatial resolution of the 3D sequence scan, which is susceptible to motion artifacts (27,28), the plaque signal at some levels may be disturbed by this motion artifact. Finally, while we strictly followed the bilateral renal artery openings to local the radiologic-pathologic correlations, the thickness of the pathological sections was significantly smaller than the layer thickness of the MRI scans, so the radiologic-pathologic correlations inevitably had some errors.

Conclusions

In this study, we used VWMRI to investigate the development of plaque changes in a rabbit model of abdominal aortic atherosclerosis and found that VWMRI can be used to qualitatively and quantitatively assess plaque changes before and after a lipid-lowering treatment with atorvastatin. Further, the VWMRI results had a good accord with the pathological results. As a non-invasive imaging method, VWMRI can be useful for experimental studies on the pathogenesis, diagnosis, and treatment of atherosclerotic lesions.

Acknowledgments

Funding: The project was funded by the Natural Science Foundation of Liaoning Province (No. 2019-ZD-0762).

Footnote

Reporting Checklist: The authors have completed the ARRIVE reporting checklist. Available at <https://atm.amegroups.com/article/view/10.21037/atm-22-1263/rc>

Data Sharing Statement: Available at <https://atm.amegroups.com/article/view/10.21037/atm-22-1263/dss>

Conflicts of Interest: All authors have completed the ICMJE uniform disclosure form (available at <https://atm.amegroups.com/article/view/10.21037/atm-22-1263/coif>). The authors have no conflicts of interest to declare.

Ethical Statement: The authors are accountable for all aspects of the work in ensuring that questions related to the accuracy or integrity of any part of the work are appropriately investigated and resolved. This experiment

was performed under a project license (No. EC-2019-KS-016) granted by the ethics committee of The Fourth Affiliated Hospital of China Medical University, in compliance with Chinese guidelines for the care and use of animals.

Open Access Statement: This is an Open Access article distributed in accordance with the Creative Commons Attribution-NonCommercial-NoDerivs 4.0 International License (CC BY-NC-ND 4.0), which permits the non-commercial replication and distribution of the article with the strict proviso that no changes or edits are made and the original work is properly cited (including links to both the formal publication through the relevant DOI and the license). See: <https://creativecommons.org/licenses/by-nc-nd/4.0/>.

References

1. Harloff A, Simon J, Brendecke S, et al. Complex plaques in the proximal descending aorta: an underestimated embolic source of stroke. *Stroke* 2010;41:1145-50.
2. Sen S, Hinderliter A, Sen PK, et al. Aortic arch atheroma progression and recurrent vascular events in patients with stroke or transient ischemic attack. *Circulation* 2007;116:928-35.
3. Liu M, Wu B, Wang WZ, et al. Stroke in China: epidemiology, prevention, and management strategies. *Lancet Neurol* 2007;6:456-64.
4. Mazzacane F, Mazzoleni V, Scola E, et al. Vessel Wall Magnetic Resonance Imaging in Cerebrovascular Diseases. *Diagnostics (Basel)* 2022;12:258.
5. Chaganti J, Woodford H, Tomlinson S, et al. Black blood imaging of intracranial vessel walls. *Pract Neurol* 2020. [Epub ahead of print].
6. Mandell DM, Mossa-Basha M, Qiao Y, et al. Intracranial Vessel Wall MRI: Principles and Expert Consensus Recommendations of the American Society of Neuroradiology. *AJNR Am J Neuroradiol* 2017;38:218-29.
7. Tan HW, Chen X, Maingard J, et al. Intracranial Vessel Wall Imaging with Magnetic Resonance Imaging: Current Techniques and Applications. *World Neurosurg* 2018;112:186-98.
8. Shi MC, Wang SC, Zhou HW, et al. Compensatory remodeling in symptomatic middle cerebral artery atherosclerotic stenosis: a high-resolution MRI and microemboli monitoring study. *Neurol Res* 2012;34:153-8.
9. Yanni AE. The laboratory rabbit: an animal model of

- atherosclerosis research. *Lab Anim* 2004;38:246-56.
10. Fan J, Kitajima S, Watanabe T, et al. Rabbit models for the study of human atherosclerosis: from pathophysiological mechanisms to translational medicine. *Pharmacol Ther* 2015;146:104-19.
 11. Samuels OB, Joseph GJ, Lynn MJ, et al. A standardized method for measuring intracranial arterial stenosis. *AJNR Am J Neuroradiol* 2000;21:643-6.
 12. Qiao Y, Anwar Z, Intrapiromkul J, et al. Patterns and Implications of Intracranial Arterial Remodeling in Stroke Patients. *Stroke* 2016;47:434-40.
 13. Xu WH, Li ML, Gao S, et al. Plaque distribution of stenotic middle cerebral artery and its clinical relevance. *Stroke* 2011;42:2957-9.
 14. Turan TN, LeMatty T, Martin R, et al. Characterization of intracranial atherosclerotic stenosis using high-resolution MRI study--rationale and design. *Brain Behav* 2015;5:e00397.
 15. Yamagishi M, Terashima M, Awano K, et al. Morphology of vulnerable coronary plaque: insights from follow-up of patients examined by intravascular ultrasound before an acute coronary syndrome. *J Am Coll Cardiol* 2000;35:106-11.
 16. Fan J, Chen Y, Yan H, et al. Principles and Applications of Rabbit Models for Atherosclerosis Research. *J Atheroscler Thromb* 2018;25:213-20.
 17. Emini Veseli B, Perrotta P, De Meyer GRA, et al. Animal models of atherosclerosis. *Eur J Pharmacol* 2017;816:3-13.
 18. Gargiulo S, Gramanzini M, Mancini M. Molecular Imaging of Vulnerable Atherosclerotic Plaques in Animal Models. *Int J Mol Sci* 2016;17:1511.
 19. Shiomi M, Koike T, Ito T. Contribution of the WHHL rabbit, an animal model of familial hypercholesterolemia, to elucidation of the anti-atherosclerotic effects of statins. *Atherosclerosis* 2013;231:39-47.
 20. Rosenson RS. Pluripotential mechanisms of cardioprotection with HMG-CoA reductase inhibitor therapy. *Am J Cardiovasc Drugs* 2001;1:411-20.
 21. Bustos C, Hernández-Presa MA, Ortego M, et al. HMG-CoA reductase inhibition by atorvastatin reduces neointimal inflammation in a rabbit model of atherosclerosis. *J Am Coll Cardiol* 1998;32:2057-64.
 22. Shi Z, Zhu C, Degnan AJ, et al. Identification of high-risk plaque features in intracranial atherosclerosis: initial experience using a radiomic approach. *Eur Radiol* 2018;28:3912-21.
 23. Feig JE, Feig JL, Kini AS. Statins, atherosclerosis regression and HDL: Insights from within the plaque. *Int J Cardiol* 2015;189:168-71.
 24. Gupta A, Baradaran H, Al-Dasuqi K, et al. Gadolinium Enhancement in Intracranial Atherosclerotic Plaque and Ischemic Stroke: A Systematic Review and Meta-Analysis. *J Am Heart Assoc* 2016;5:003816.
 25. Calcagno C, Lairez O, Hawkins J, et al. Combined PET/DCE-MRI in a Rabbit Model of Atherosclerosis: Integrated Quantification of Plaque Inflammation, Permeability, and Burden During Treatment With a Leukotriene A4 Hydrolase Inhibitor. *JACC Cardiovasc Imaging* 2018;11:291-301.
 26. Calcagno C, Vucic E, Mani V, et al. Reproducibility of black blood dynamic contrast-enhanced magnetic resonance imaging in aortic plaques of atherosclerotic rabbits. *J Magn Reson Imaging* 2010;32:191-8.
 27. Ryu CW, Jahng GH, Kim EJ, et al. High resolution wall and lumen MRI of the middle cerebral arteries at 3 tesla. *Cerebrovasc Dis* 2009;27:433-42.
 28. Bodle JD, Feldmann E, Swartz RH, et al. High-resolution magnetic resonance imaging: an emerging tool for evaluating intracranial arterial disease. *Stroke* 2013;44:287-92.

Cite this article as: Wu Y, Li F, Wang Y, Hu T, Gao L. Lipid-lowering treatment in a rabbit model of atherosclerosis: a vessel wall magnetic resonance imaging study. *Ann Transl Med* 2022;10(10):569. doi: 10.21037/atm-22-1263